Journal of Inorganic and General Chemistry
ZAAC
Zeitschrift für anorganische und allgemeine Chemie
DOI: 10.1002/zaac.201900141
ARTICLE

New Homoleptic Rare-Earth Metal Complexes Comprising the Unsymmetrically Substituted Amidinate Ligand [MeC(NEt)(N*t*Bu)]$^-$

Nicole Harmgarth,[a] Phil Liebing,[a] Liane Hilfert,[a] Volker Lorenz,[a] Felix Engelhardt,[a] Sabine Busse,[a] and Frank T. Edelmann*[a]

Dedicated to Professor Klaus Jacob on the Occasion of his 80th Birthday

Abstract. New homoleptic complexes of selected rare-earth elements containing the unsymmetrically substituted amidinate ligand [MeC(NEt)(N*t*Bu)]$^-$ [= (L)$^-$] were synthesized and fully characterized. Treatment of in situ-prepared Li(L) (**1**) with anhydrous lanthanide(III) chlorides, *Ln*Cl$_3$ (*Ln* = Sc, La, Ce, Ho), afforded three different types of amidinate complexes depending on the ionic radius of the central metal atom. The large La^{3+} formed the octa-coordinate DME solvate La(L)$_3$(DME) (**2**). Using Ce^{3+}, the octa-coordinate "ate" complex Li(THF)[Ce(L)$_4$] (**3**) was formed. Depending on the crystallization conditions, compound **3** could be crystallized in two modifications differing in the coordination environment around Li. In the case of the smaller Sc^{3+} and Ho^{3+} ions, six-coordinate homoleptic Sc(L)$_3$ (**4**) and Ho(L)$_3$ (**5**) were isolated. The title compounds were fully characterized by spectroscopic and analytical methods as well as single-crystal X-ray diffraction. With *Ln* = La and Ce, several by-products incorporating lithium, chlorine and/or oxygen were also isolated and structurally characterized.

Introduction

Anionic 1,3-diazaallyl-type chelating ligands like the amidinates, [RC(NR′)$_2$]$^-$, and guanidinates, [R$_2$NC(NR′)$_2$]$^-$, form stable and potentially useful complexes with nearly every metallic element in the Periodic Table.[1–8] Amidinate and guanidinate complexes have found numerous practical applications, particularly in the areas of homogeneous catalysis and materials science.[9,10] Many of them are promising homogeneous catalysts e.g. for olefin polymerization and hydroamination reactions,[11–15] whereas certain alkyl-substituted complexes are sufficiently volatile to be useful precursors for ALD (atomic layer deposition) and CVD (chemical vapor deposition) processes.[16–24] Recent contributions to this field clearly revealed that the use of *unsymmetrically substituted* amidinate and guanidinates ligands leads to further improved volatility of the respective transition metal and lanthanide complexes. For example, replacement of the chelating guanidinate ligand in the tantalum(V) tetraamide precursor Ta(NMe$_2$)$_4$[Me$_2$NC(N*i*Pr)$_2$] by the asymmetric ligand [Me$_2$NC(NEt)(N*t*Bu)]$^-$ led to the significantly more volatile isomer Ta(NMe$_2$)$_4$[Me$_2$NC(NEt)(N*t*Bu)].[25] Similarly, the new volatile cobalt(II) amidinates Co[RC(N*t*Bu)(NEt)]$_2$ (R = Me, Et, *n*Bu) were found to evaporate cleanly without decomposition. Two of them are even liquids at room temperature, allowing for highly convenient preparation, handling and purification by distillation. All three are highly reactive compounds which are suitable precursors for vapor deposition of cobalt metal, cobalt nitride and cobalt oxide.[26] In lanthanide precursor chemistry, the homoleptic gadolinium tris(amidinate) complex Gd(L)$_3$ (L = [MeC(NEt)(N*t*Bu)]$^-$) also exhibited significantly improved volatility. Gd(L)$_3$ was successfully employed in the MOCVD production of gadolinium nitride (GdN) thin layers.[27]

In this context we recently investigated the chemistry of the unsymmetrically substituted lithium amidinate reagent Li(L) (**1**), which can be prepared by treatment of 1-*tert*-butyl-3-ethyl-carbodiimide, *t*Bu-N=C=N-Et, with methyllithium in ether-type solvents. Clean formation of **1** was observed when the reaction was carried out in Et$_2$O/THF mixtures while the same preparations on pure diethyl ether or DME (= 1,2-dimethoxyethane) resulted in formation of unexpected hepta- and octanuclear lithium amidinate clusters. Treatment of anhydrous praseodymium(III) chloride with in situ-prepared **1** in Et$_2$O/THF afforded green Li(THF)[Pr(L)$_4$] as the first tetrakis(amidinato)lanthanide(III) complex in 55% isolated yield.[28] We now report an extension of this chemistry to other rare-earth metals and the structural differences of the resulting amidinate complexes depending on the ionic radii of the central metals.

Results and Discussion

Preparation and Properties

The synthetic route to the title compounds always starts with the preparation of the unsymmetrically substituted amidinate

* Prof. Dr. F. T. Edelmann
Fax: +49-391-67-12933
E-Mail: frank.edelmann@ovgu.de
http://www.ich.ovgu.de/Lehrstühle/Anorganische+Chemie.html
[a] Chemisches Institut
Otto-von-Guericke-Universität Magdeburg
Universitätsplatz 2
39106 Magdeburg, Germany

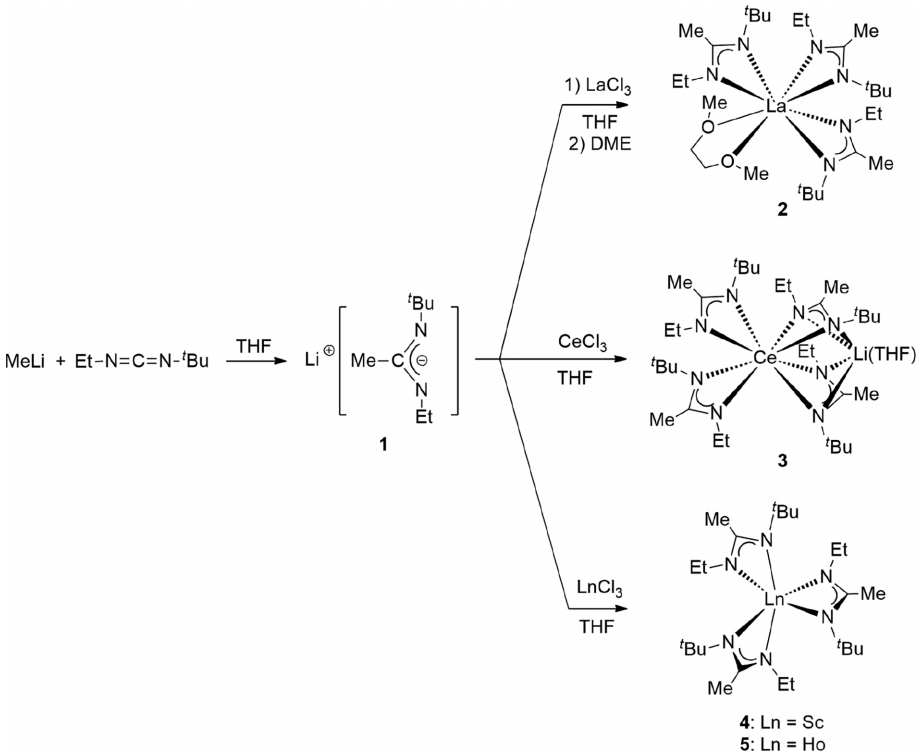

Scheme 1. Preparation of the rare-earth amidinates **2**–**5**.

precursor Li(L) (**1**), which is easily made in situ by treatment of 1-*tert*-butyl-3-ethyl-carbodiimide, *t*Bu-N=C=N–Et, with 1 equiv. of methyllithium in THF. The resulting clear solutions of **1** were then treated with anhydrous chlorides of trivalent rare-earth metals, $LnCl_3$ (*Ln* = Sc, La, Ce, Ho), in a molar ratio of 3:1. As shown in Scheme 1, the outcome of these reactions was dependent on the ionic radii of the respective lanthanide ions. In the case of the largest ion in the series, La^{3+},[29] three amidinate ligands are not sufficient to saturate the coordination sphere around lanthanum, so that an octa-coordinate DME solvate of the composition $La(L)_3(DME)$ (**2**) was isolated as colorless, moisture-sensitive crystals. The reaction of **1** with anhydrous cerium(III) chloride in a stoichiometric ratio of 3:1 provided small amounts of the pale yellow tetrakis(amidinato) cerium(III) complex $Li(THF)[Ce(L)_4]$ (**3**). Significantly better yields of **3** were achieved by adjusting the molar ratio of the reactants to 4:1. Similar reactions with the smaller metal ions Sc^{3+} and Ho^{3+} afforded the unsolvated, homoleptic complexes $Sc(L)_3$ (**4**, colorless crystals) and $Ho(L)_3$ (**5**, yellow crystals). Isolated yields of compounds **2**–**5** were in the rather low range of 32–48 %, which can be traced back to the very high solubility even in non-polar organic solvents such as *n*-pentane and toluene.

The target products **2**–**5** were fully characterized by the usual set of analytical methods. In all cases, elemental analyses (C, H, N) confirmed the composition of the products. Mass spectra of the homoleptic derivatives **4** and **5** showed the molecular ions $[Ln(L)_3]^+$ (*Ln* = Sc, Ho) at *m*/*z* 468 (rel. int. 17 %) (**4**) and 588 (rel. int. 16 %) (**5**), respectively. Notably, the $[Ln(L)_3]^+$ ions also gave rise to the highest peaks in the mass spectra of **2** (*m*/*z* 562, rel. int. 50 %) and **3** (*m*/*z* 563, rel. int. 87 %). Various bands attributable to aliphatic C–H vibrations were assigned in the IR spectra of **2**–**5** (see Experimental Section). Moreover, weak but characteristic ν(NCN) bands were observed in the spectra of **2** (1655 cm^{-1}) and **5** (1644 cm^{-1}). The coordinated solvents in **2** and **3** gave rise to ν_{as}(C–O–C) bands at 1149 (m) cm^{-1} and 1125 (vs) cm^{-1}, respectively. A very strong band at 370 cm^{-1} in the IR spectrum of **4** could be assigned to the ν(Sc–N) vibration.

Interpretable ^1H and ^{13}C NMR spectroscopic data could be obtained for the complexes **2**–**4**, whereas the strongly paramagnetic character of the Ho^{3+} ion precluded the measurement of meaningful NMR spectra in the case of compound **5**. All other NMR spectroscopic data were in good agreement with the proposed structures, clearly showing the presence of DME in **2** and THF in **3**. The formation of a pure scandium species was corroborated by the presence of a single resonance at δ = 208 ppm in the ^{45}Sc NMR spectrum of **4**. This is in good agreement with the ^{45}Sc NMR resonance of the closely related homoleptic scandium guanidinate complex $Sc[c\text{-}C_2H_4N\text{–}C(NiPr)_2]_3$ (*c*-C_2H_4N = aziridyl), which was found at δ = 203 ppm.[30]

Crystal Structures

The molecular and crystal structures of three title compounds (**2**, **3**, and **5**) were determined by single-crystal X-ray diffraction studies (Table 1). Only the scandium complex **4** resisted all attempts to grow X-ray-quality single-crystals from various solvents (DME, Et_2O, toluene, *n*-pentane). All three

Table 1. Crystallographic data for compounds **2**, **3** and **5**.

	2	**3-oP**	**3-oF**	**5**
Chemical formula	$C_{28}H_{61}LaN_6O_2$	$C_{36}H_{76}CeLiN_8O$	$C_{36}H_{76}CeLiN_8O$	$C_{24}H_{51}HoN_6$
Formula weight /g·mol^{-1}	652.73	784.10	784.10	588.63
Crystal color and shape	colorless blocks	colorless blocks	colorless blocks	light yellow rods
Crystal system	monoclinic	orthorhombic	orthorhombic	monoclinic
Space group	$P2_1/n$	*Pbca*	*Fdd2*	$P2_1/n$
Unit cell parameters				
a /Å	11.184(4)	18.524(3)	25.7922(6)	9.5045(3)
b /Å	29.744(9)	19.294(3)	29.2182(9)	19.6082(6)
c /Å	11.179(4)	23.610(4)	23.1550(5)	15.6577(5)
α /°	90	90	90	90
β /°	115.88(3)	90	90	99.912(2)
γ /°	90	90	90	90
Unit cell volume /Å^3	3346(2)	8438(2)	17449.6(8)	2874.5(2)
Molecules per cell Z	4	8	16	4
Electrons per cell F(000)	1376	3336	6672	1216
Calcd. density ρ /g·cm^{-3}	1.296	1.234	1.194	1.360
μ (Mo-K_α) /mm^{-1}	1.308	1.114	1.078	2.773
Crystal size /mm	0.24 × 0.18 × 0.13	0.21 × 0.14 × 0.09	0.37 × 0.28 × 0.23	0.25 × 0.10 × 0.09
T /K	100(2)	100(2)	153(2)	153(2)
θ range /°	2.137.. 27.098	1.751···25.200	2.245···26.166	2.342···24.995
Reflections collected	17657	62916	16657	15839
Reflections unique	7190	7586	8470	5061
Reflections with $I > 2\sigma(I)$	6215	7120	7811	4177
Completeness of dataset	96.7 %	99.9 %	99.8 %	99.9 %
R_{Int}	0.0628	0.0469	0.0228	0.0761
Parameters / Restraints	693 / 1805	444 / 0	444 / 23	316 / 0
R_1 [all data; I>2 σ (I)]	0.0599; 0.0473	0.0388; 0.0355	0.0266; 0.0224	0.0559; 0.0413
wR_2 [all data; I>2 σ (I)]	0.1011; 0.0967	0.0626; 0.0615	0.0454; 0.0446	0.0939; 0.0889
GooF (F^2)	1.127	1.286	1.004	1.090
Extinction coefficient	–	–	–	0.0010(2)
Largest diff. peak and hole /e·Å^{-3}	0.801; –1.648	0.375; –0.558	0.276; –0.446	0.754; –1.182
Flack parameter	–	–	–0.015(6)	–

compounds **2**, **3**, and **5** exist as well-defined monomeric molecules with one formula moiety in the asymmetric unit. The coordination of the central lanthanum atom in **2** can be described as distorted square-antiprismatic with N1–N4–N3–N6 and N2–N5–O2–O1 defining the base areas [angle between planes = 21(2)°]. The La–N bond lengths are in a range of 249.0(6)–269.6(7) pm, which is within the range of La–N distances observed for other octa-coordinate lanthanum complexes with nitrogen ligands (Figure 1).[31]

Depending on the crystallization conditions, compound **3** could be crystallized in two modifications differing in the coordination environment around Li. Colorless crystals of an orthorhombic primitive modification (**3-oP**; space group *Pbca*) were grown over a few days by carefully layering a concentrated solution of **3** in THF with *n*-pentane. Recrystallization of **3** from diethyl ether resulted in colorless block-like crystals of an orthorhombic face-centered modification (**3-oF**; space group *Fdd2*) The coordination environments of the cerium in both modifications of **3** are very similar and resemble that in **2**, with the DME ligand being formally replaced by a fourth amidinate ligand (Figure 2). The angles between the base areas of the distorted square antiprism are 17.4(1)° (**3-oP**) and 15.4(1)° (**3-oF**), respectively. The Ce–N separations are also almost identical in both forms. Seven Ce–N bonds are in a range of 252.4(2)–271.1(2) pm (**3-oP**) or 252.7(3)–278.5(4) pm (**3-oF**), respectively, whereas one bond (Ce-N6) is markedly elongated

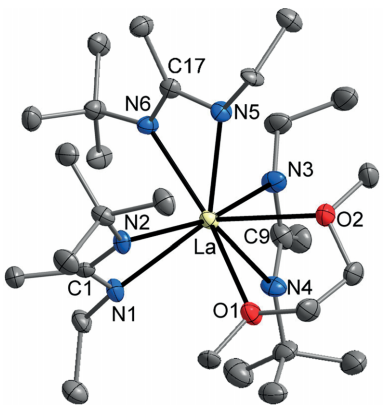

Figure 1. Molecular structure of La(L)$_3$(DME) (**2**) in the crystalline state. Displacement ellipsoids of the heavier atoms with 50 % probability, hydrogen atoms and disorder of amidinate and DME ligands are omitted for clarity. Selected interatomic distances /pm: La–N1 251.9(6), la–N2 259.2(6), La–N3 256.1(7), La–N4 269.6(7), La–N5 249.0(6), La–N6 250.9(7), La–N1' 250.6(6), La–N2' 259.9(6), La–N3' 249.4(6), La–N4' 250.6(6), La–N5' 254.9(7), La–N6' 268.9(7), La–O1 272.5(6), La–O2 275.0(5), La–O1' 272.0(6), La–O2' 276.0(5).

to 297.2(2) pm (**3-oP**) or 293.8(3) pm (**3-oF**). Ce–N bond lengths in octa-coordinate cerium complexes are usually between 235 and 280 pm,[31] and therefore compound **3** should be regarded as an intermediate case between seven- and eight-coordinate cerium.

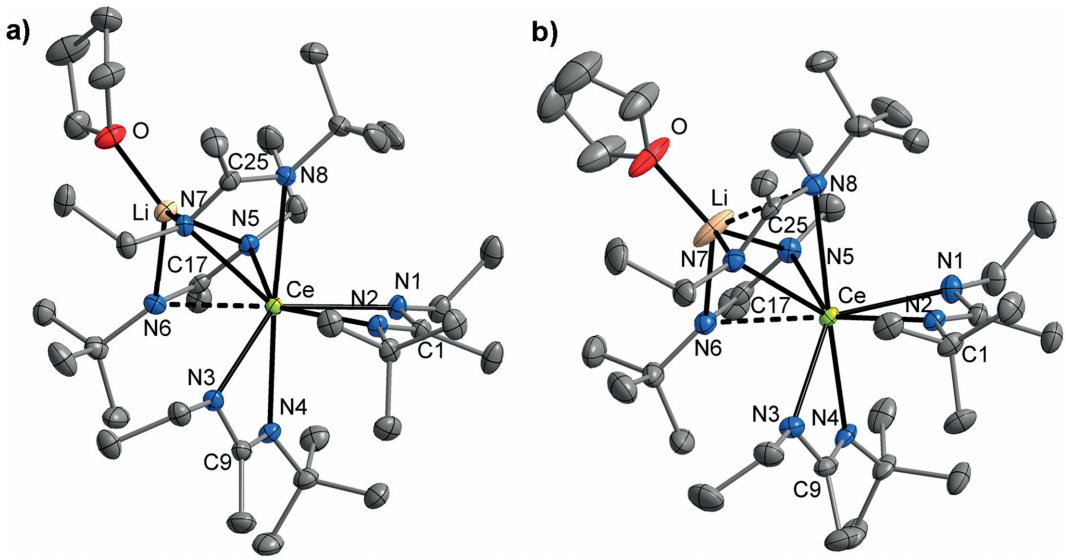

Figure 2. Molecular structures of two different modifications of Li(THF)[Ce(L)$_4$] (**3**) in the crystal: a) orthorhombic primitive (**3-oP**; space group *Pbca*) and b) orthorhombic face-centered (**3-oF**; space group *Fdd2*). Displacement ellipsoids of the heavier atoms with 50 % probability, hydrogen atoms are omitted for clarity. Selected interatomic distances /pm: **3–oP**: Ce1–N1 255.0(2), Ce1–N2 252.4(2), Ce1–N3 255.0(2), Ce1–N4 256.8(2), Ce1–N5 254.8(2), Ce1–N6 297.7(2), Ce1–N7 260.0(2), Ce1–N8 271.1(2), Li1–N5 215.4(5), Li1–N6 203.2(5), Li1–N7 205.9(5), Li1–O1 193.1(5); **3–oF**: Ce–N1 256.1(3), Ce–N2 252.7(3), Ce–N3 254.8(3), Ce–N4 252.8(3), Ce–N5 257.9(3), Ce–N6 293.8(3), Ce–N7 259.5(3), Ce–N8 278.5(4), Li–N5 219(1), Li–N6 216(1), Li–N7 210(1), Li–N8 264(1), Li–O 192(1).

The most significant difference between the two polymorphic forms of **3** is the coordination environment of the lithium atom. While the latter in **3-oP** displays a typical tetrahedral coordination by three amidinate nitrogen atoms and one THF ligand, the coordination in **3-oF** is extended to distorted square-pyramidal by an additional Li···N contact of 264(1) pm. The significance of the latter is reflected by the elongation of the other Li–N bonds going from **3-oP** (203.2(5)–215.4(5) pm) to **3-oF** (210(1)–219(1) pm). The modification **3-oF** is isotypic with the previously reported crystal structure of the analog praseodymium complex Li(THF)[Pr(L)$_4$].[28]

The central holmium atom in **5** displays a distorted-octahedral coordination with N–Ho–N(*trans*) angles in a range of 150.3(2)–154.7(2)° (Figure 3). Different from the high-coordinate complexes **2** and **3**, the *Ln*–N bond lengths in **5** are in a much narrower range of 233.4(4)–236.8(5) pm. These values are relatively small as compared to those observed in the related binary holmium amidinate Ho[*c*Pr–C≡C–C(N*i*Pr)$_2$]$_3$ [Ho–N 234.2(2)–238.3(3) pm][32] and in the guanidinate Ho[*c*–C$_2$H$_4$N–C(N*i*Pr)$_2$]$_3$ [Ho–N 234.8(3)–239.6(3) pm].[30] The range of Ho–N distances usually observed in hexa-coordinate complexes is 230–260 pm.[31] Worth mentioning, **5** is isotypic with the earlier reported gadolinium analog Gd(L)$_3$.[27]

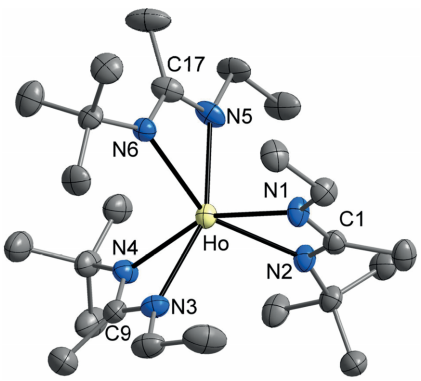

Figure 3. Molecular structure of Ho(L)$_3$ (**5**) in the crystal. Displacement ellipsoids of the heavier atoms with 40 % probability, hydrogen atoms are omitted for clarity. The ethyl group attached to N5 is disordered over two orientations (only one orientation shown). Selected interatomic distances /pm: Ho–N1 233.4(4), Ho–N2 236.2(5), Ho–N3 234.6(5), Ho–N4 236.7(4), Ho–N5 234.1(5), Ho–N6 236.8(5).

Formation of Cl- or O-containing By-products

All compounds described in this study are highly sensitive to moisture due to the pronounced oxophilicity of the rare-earth metals. Moreover, it is well-established that in homologous series of (organo)lanthanide(III) complexes the cerium derivatives are often also sensitive towards oxidation.[33] Occasionally, during the syntheses of the title compounds according to Scheme 1, small amounts of well-formed crystals of by-products were isolated, which could be structurally characterized through X-ray diffraction. The compounds have been numbered as **S1**–**S4** (Scheme 2), and their structural characterization by X-ray diffraction is reported (Table 2). Two complexes of the composition $Ln^{III}_2Li_2(\mu_4\text{-O})(L)_6$ (**S1**: *Ln* = La; **S2**: *Ln* = Ce) were obtained during the preparation of **2** and **3**, respectively, which were most likely formed due to the presence of trace amounts of water in the reaction mixtures. Red $Ce^{IV}_3(\mu\text{-O})_3(L)_6$ (**S3**) is certainly the product of contamination with oxygen, as it contains cerium in the tetravalent oxidation state. In contrast, bright yellow $Ce^{III}_2(\mu\text{-Cl})(\mu\text{-L})(L)_4$ (**S4**) ob-

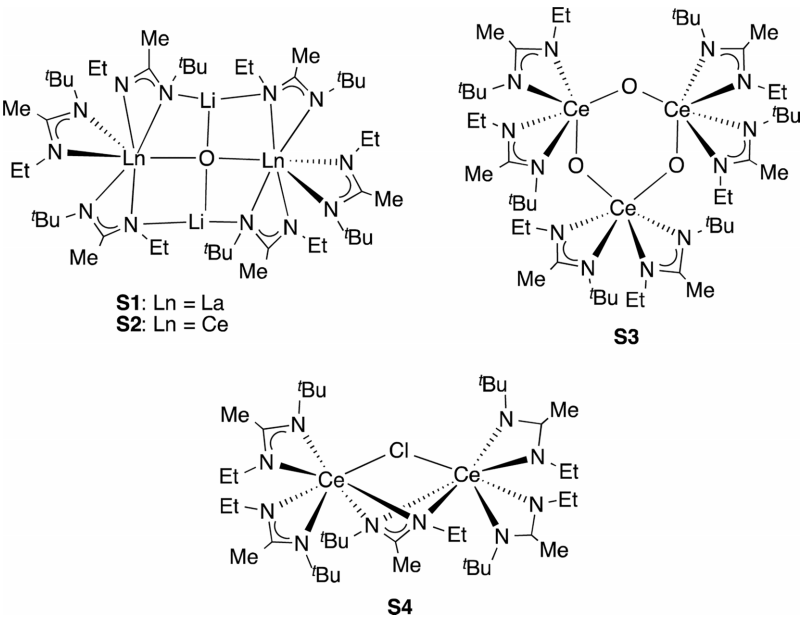

Scheme 2. Schematic representation of the serendipitously observed by-products **S1**–**S4**.

Table 2. Crystallographic data for compounds **S1**–**S4**.

	S1	**S2**	**S3**	**S4**
Chemical formula	$C_{48}H_{102}La_2Li_2N_{12}O$	$C_{48}H_{102}Ce_2Li_2N_{12}O$ [a]	$C_{48}H_{102}Ce_3N_{12}O_3$	$C_{40}H_{85}Ce_2ClN_{10}$
Formula weight /g·mol^{-1}	1155.11	1157.53 [a]	1315.77	1021.86
Crystal color and shape	colorless blocks	orange blocks	red needles	yellow plates
Crystal system	tetragonal	monoclinic	monoclinic	triclinic
Space group	$P4_32_12$	$P2_1/c$	$C2/c$	$P\bar{1}$
Unit cell parameters				
a /Å	12.887(3)	40.058(1)	11.026(5)	9.3993(3)
b /Å	= a	15.0782(3)	24.86(2)	14.5265(4)
c /Å	35.447(11)	20.1171(6)	22.24(1)	19.4929(5)
α /°	90	90	90	81.180(2)
β /°	90	95.102(2)	92.04(3)	85.532(2)
γ /°	90	90	90	72.350(2)
Unit cell volume /Å^3	5886(3)	12102.5(5)	6092(5)	2504.9(1)
Molecules per cell Z	4	8	4	2
Electrons per cell F(000)	2408	4832 [a]	2688	1056
Calcd. density ρ /g·cm^{-3}	1.303	1.271 [a]	1.435	1.355
μ (Mo-K_α) /mm^{-1}	1.474	1.526 [a]	2.249	1.883
Crystal size /mm	0.17 × 0.15 × 0.10	0.36 × 0.30 × 0.19	0.16 × 0.08 × 0.03	0.19 × 0.17 × 0.11
T /K	100(2)	153(2)	100(2)	153(2)
θ range /°	1.954.. 29.169	1.927···25.000	1.877···25.248	2.116···27.000
Reflections collected	18147	59898	14270	28768
Reflections unique	7758	21079	5480	10922
Reflections with $I > 2\sigma(I)$	7278	16399	4980	9118
Completeness of dataset	97.6 %	99.0 %	99.1 %	100 %
R_{Int}	0.0848	0.0594	0.0475	0.0352
Parameters / Restraints	309 / 538	1232 / 0	332 / 588	503 / 0
R_1 [all data; I>2 σ (I)]	0.0632; 0.0579	0.0699; 0.0517	0.0398; 0.0354	0.0376; 0.0254
wR_2 [all data; I>2 σ (I)]	0.1459; 0.1419	0.1266; 0.1212	0.0934; 0.0910	0.0482; 0.0457
GooF (F^2)	1.119	1.103	1.030	0.986
Extinction coefficient	–	0.00070(3)	–	–
Largest diff. peak and hole /e·Å^{-3}	1.279; –1.653	–	1.393; –1.062	0.445; –0.776
Flack parameter	–0.03(3)	–	–	–

a) Without solvent of crystallization. Diffuse solvent electron density was considered using the SQUEEZE routine of Platon[42].

viously resulted from incomplete substitution of the chloride ions in $CeCl_3$ by amidinate ligands.

The molecular structures of the heterometallic complexes **S1** and **S2** are very similar, but the crystal symmetries are entirely

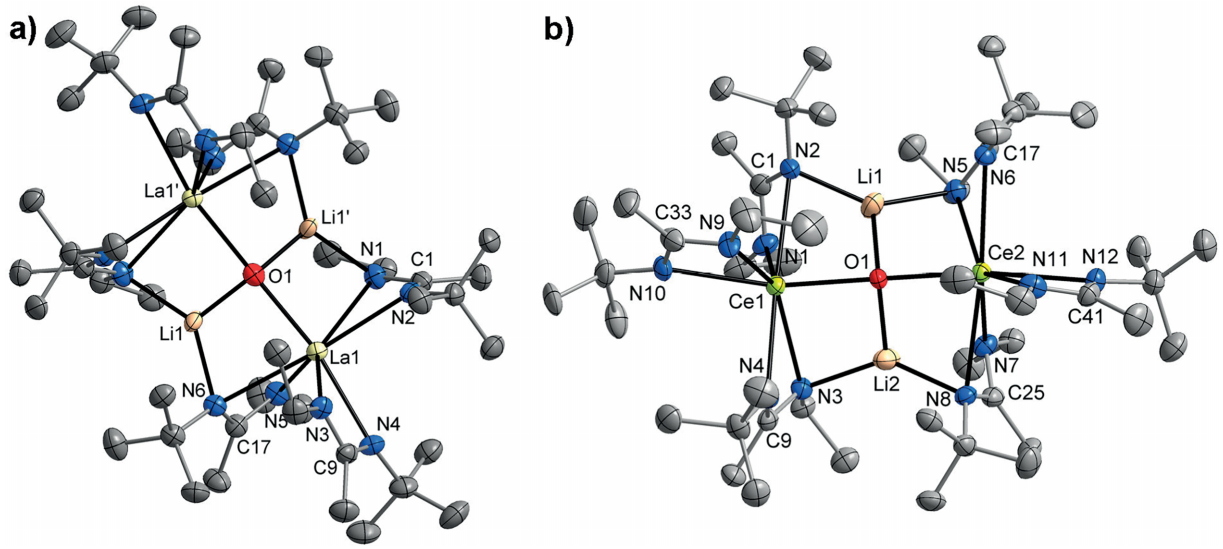

Figure 4. Molecular structures of (a) $La_2Li_2(\mu_4\text{-}O)(L)_6$ (**S1**) and (b) $Ce_2Li_2(\mu_4\text{-}O)(L)_6$ (**S2**; one of two molecules in the asymmetric unit) in the crystal. Displacement ellipsoids drawn at the 50 % probability level, hydrogen atoms are omitted for clarity. Selected interatomic distances /pm: **S1**: La1–N1 270.1(7), La1–N2 262.4(7), La1–N3 257.6(7), La1–N4 258.6(7), La1–N5 259.4(7), La1–N6 274.6(7), La1–O1 231.9(1), Li1–N1' 201.6(2), Li1–N6 203.6(2), Li1–O1 189.6(1); **S2**: Ce1–N1 256.7(6), Ce1–N2 277.0(6), Ce1–N3 264.5(5), Ce1–N4 261.3(6), Ce1–N9 250.8(5), Ce1–N10 256.8(5), Ce2–N5 266.8(5), Ce2–N6 259.1(6), Ce2–N7 258.0(5), Ce2–N8 273.7(6), Ce2–N11 253.5(5), Ce2–N12 256.7(6), Ce1–O1 226.7(4), Ce2–O1 227.1(4), Li1–N2 199.2(1), Li1–N5 202.3(2), Li2–N3 202.3(1), Li2–N8 202,8(1), Li1–O1 190.8(1), Li2–O1 191.4(1).

different. In **S1**, the central oxygen atom is situated on a two-fold rotational axis, whereas the asymmetric unit in **S2** contains two molecules together with diffuse solvent of crystallization (Figure 4). Four out of six amidinate ligands adopt a κ*N*,κ*N*′:κ*N*-bridging coordination between a lanthanide and a lithium atom, whereas the remaining two amidinate ligands are attached to the lanthanide in a typical chelating mode. With other words, two lanthanide(III) amidinate units, *Ln*(L)$_3$, are linked by a molecular Li_2O moiety, resulting in a "mesh network" of four edge-linked *Ln*LiNO rings. The lanthanide atoms are seven-coordinate in an irregular fashion, whereas lithium adopts a somewhat trigonal-planar coordination [sum of coordination angles 358.5(8)° for **S1** and 353.2(8)–359.9(8)° for **S2**]. The coordination of the central oxide ligand strongly differs from an ideal tetrahedron, with *Ln*–O–*Ln* angles being close to linearity at 172.0(4)° (**S1**) and 172.3(2)–175.3(2)° (**S2**). "Li_2O adducts" of rare-earth complexes that are structurally related to **S1** and **S2** have been reported earlier, namely with yttrium,[34] dysprosium,[35] and ytterbium.[36]

The cerium(IV) complex **S3** is formally a cyclic trimer of $CeO(L)_2$ units, featuring a planar Ce_3O_3 ring, which is slightly prolated along the Ce2–O2 vector (Figure 5). The molecular symmetry is therefore C_{2v}. A distorted octahedral coordination of the cerium atoms is completed by each two chelating amidinate ligands. The tetravalent nature of the cerium atom is confirmed by the Ce–N separations being relatively small at 242.5(4)–246.4(3) pm, whereas the Ce–N bond lengths observed for cerium(III) amidinates and guanidinates are usually in a range of 246–256 pm.[31] Cerium(IV) amidinates and guanidinates are quite rare, with the cationic complex $[Ce\{(Me_3Si)_2N\text{-}C(N\textit{i}Pr)_2\}]^+$ as an example [Ce–N 237.4(3)–242.8(4) pm].[37] Two trinuclear cerium(IV) complexes comprising a six-membered Ce_3O_3 ring similar to **S3** have been reported earlier, $Ce_3(\mu\text{-}O)_3[N(SiMe_3)_2]_6$ [38] and $Ce_3(\mu\text{-}O)_3(\eta^5\text{-}C_5H_4\text{-}SiMe_3)_6$.[39] This structural motif seems to be characteristic for tetravalent cerium, since analogous structures with cerium(III) or other trivalent rare earths are not known to the best of our knowledge.[31]

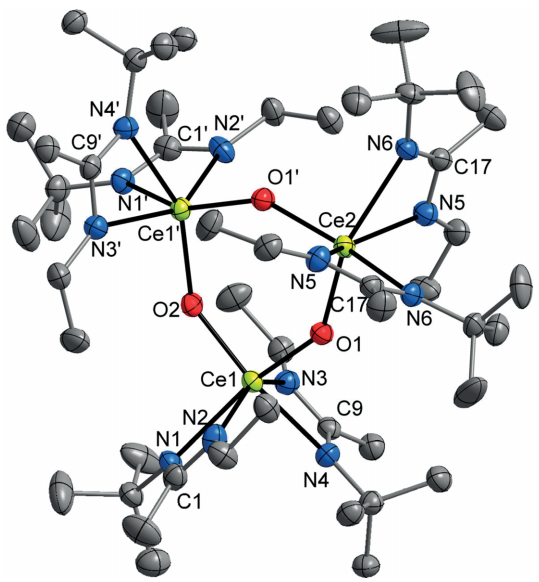

Figure 5. Molecular structure of $Ce_3(\mu\text{–}O)_3(L)_6$ (**S3**) in the crystal. Displacement ellipsoids drawn at the 50 % probability level, hydrogen atoms are omitted for clarity. Selected interatomic distances /pm: Ce1–N1 244.0(3), Ce1–N2 244.8(4), Ce1–N3 244.7(4), Ce1–N4 243.5(4), Ce2–N5 242.5(4), Ce2–N6 246.4(3), Ce1–O1 208.6(3), Ce1–O2 208.7(1), Ce2–O1 209.1(3).

The mixed chloride/amidinate complex **S4** consists of two central cerium(III) atoms that are linked by a μ-bridging chlorido ligand and a κ*N*,κ*N*′:κ*N*,κ*N*′-bridging amidinate li-

gand (Figure 6). Each of the two symmetry-independent cerium atoms is coordinatively saturated by two chelating amidinates, resulting in an irregular seven-coordination. Among a small number of structurally characterized chloride/amidinate complexes of cerium and several related complexes of other lanthanides, the molecular structure of **S4** is unique to the best of our knowledge.[31] The literature-known cerium complexes either contain a $Ce_2(\mu\text{-}Cl)_2$ ring as the central building unit,[40] or the chloride is attached to a single cerium center in a mononuclear complex.[41]

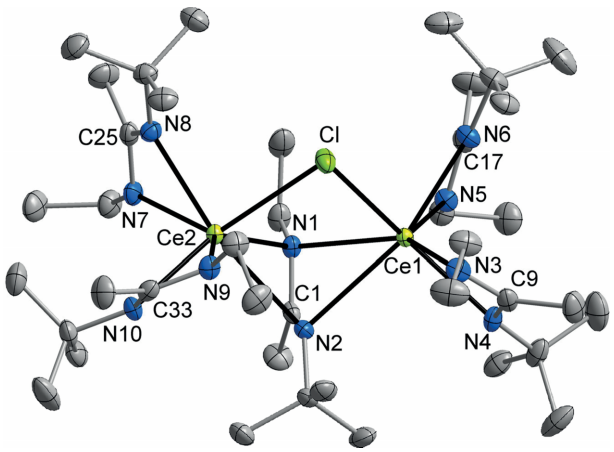

Figure 6. Molecular structure of $Ce^{III}_2(\mu\text{-}Cl)(\mu\text{-}L)(L)_4$ (**S4**) in the crystal. Displacement ellipsoids drawn at the 50 % probability level, hydrogen atoms are omitted for clarity. Selected interatomic distances / pm: Ce1–N1 262.6(2), Ce1–N2 280.2(2), Ce1–N3 247.2(2), Ce1–N4 246.5(2), Ce1–N6 248.7(2), Ce2–N1 264.4(2), Ce2–N2 275.5(2), Ce2–N7 251.6(2), Ce2–N8 248.3(2), Ce2–N9 246.8(2), Ce2–N10 247.8(2), Ce1–Cl 285.58(6), Ce2–Cl 284.79(6).

Conclusions

In summarizing the results reported herein, four new homoleptic complexes of selected lanthanide elements containing the unsymmetrically substituted amidinate ligand $[MeC(NEt)(N\mathit{t}Bu)]^-$ (= L) were synthesized and fully characterized. Treatment of in situ-prepared Li(L) (**1**) with chlorides of trivalent rare-earth metals, $\mathit{Ln}Cl_3$ (*Ln* = Sc, La, Ce, and Ho), afforded three different types of amidinate complexes depending on the ionic radius of the central metal atom. The largest lanthanide ions La^{3+} and Ce^{3+} formed the octa-coordinate complexes $La(L)_4(DME)$ (**2**) and $Li(THF)[Ce(L)_4]$ (**3**), respectively. Using the smaller Sc^{3+} and Ho^{3+} ions, six-coordinate homoleptic $Sc(L)_3$ (**4**) and $Ho(L)_3$ (**5**) were observed. Moreover, the isolation and structural characterization of a series of side products resulting from partial hydrolysis, oxidation of Ce^{III} to Ce(IV), or incomplete chloride/amidinate substitution demonstrated the manifold reactivity and high structural diversity in rare-earth amidinate chemistry. Hopefully, future work will show if these unusual complexes can be prepared in a deliberate manner.

Experimental Section

General Methods: The starting materials methyllithium (1.6 M solution in diethyl ether, Sigma–Aldrich) and 1-*tert*-butyl-3-ethyl-carbodiimide (Sigma–Aldrich) were obtained from commercial sources and used as received. Anhydrous rare-earth chlorides, $\mathit{Ln}Cl_3$ (*Ln* = Sc, La, Ce, Ho) were prepared by dehydration of the hydrated chlorides using thionyl chloride according to the literature preparation.[43] ^1H and ^{13}C NMR spectra were recorded with a Bruker DPX 400 MHz spectrometer. Chemical shifts are referenced to tetramethylsilane. IR spectra were measured with a Bruker-Optics VERTEX 70v spectrometer equipped with a diamond ATR unit between 4000 cm^{-1} and 400 cm^{-1}. Microanalysis of the compounds were performed using a "VARIO EL cube" apparatus from Elementar Analysensysteme GmbH. Melting / decomposition points were measured on a Büchi Melting Point B-540 apparatus.

X-ray Crystal Structure Analyses: Single crystal X-ray intensity data of the compounds reported in this paper were collected with a STOE IPDS 2T diffractometer equipped with a 34 cm image plate detector, using graphite-monochromated Mo-K_α radiation (λ = 0.71073 Å). Numerical absorption correction was applied on the intensity data.[44] The structures were solved with SHELXT-2015[45] and refined by full-matrix least-squares methods on F^2 using SHELXL-2016.[46] Crystallographic data and structure refinement results are listed in Table 1 and Table 2.

Crystallographic data (including structure factors) for the structures in this paper have been deposited with the Cambridge Crystallographic Data Centre, CCDC, 12 Union Road, Cambridge CB21EZ, UK. Copies of the data can be obtained free of charge on quoting the depository numbers CCDC-1853343 (**2**), CCDC-1936668 (**3-oP**), CCDC-1848870 (**3-oF**), CCDC-1853340 (**5**), CCDC-1936703 (**S1**), CCDC-1848868 (**S2**), CCDC-1848867 (**S3**), and CCDC-1848869 (**S4**) (Fax: +44-1223-336-033; E-Mail: deposit@ccdc.cam.ac.uk, http://www.ccdc.cam.ac.uk).

Preparation of the Title Compounds (General Procedure): A solution of 1-*tert*-butyl-3-ethyl-carbodiimide (1.00 g, 7.92 mmol) in THF (50 mL) was placed in a 250 mL Schlenk-flask, and 4.95 mL (7.92 mmol) of a 1.6 M solution of methyllithium in diethyl ether was added at 0 °C. After stirring at room temperature for 24 h, a suspension of the specified amount of anhydrous $\mathit{Ln}Cl_3$ in THF (50 mL) was added and stirring at room temperature was continued for 24 h (for *Ln* = La: 5 d). The reaction mixture was evaporated to dryness and the solid residue was extracted with ca. 70 mL of the specified solvent (**2**: toluene; **3** and **5**: Et_2O; **4**: *n*-pentane/toluene 10:1). After removal of the LiCl by-product by filtration, the clear filtrate was evaporated to dryness and the crude product was recrystallized from ca. 3–5 mL of the specified solvent at –32 °C (**2**: DME, **3** and **5**: Et_2O, **4**: toluene).

La(L)$_3$(DME) (2): From 0.65 g (2.64 mmol) $LaCl_3$. Yield of colorless, block-like crystals: 0.83 g (48 %). M.p. 114 °C (dec.). $C_{28}H_{61}LaN_6O_2$ (652.73 g·mol^{-1}): calcd. C 51.52; H 9.42; N 12.88 %; found: C 51.44; H 9.43; N 12.99 %. **^{1}H NMR** (400.1 MHz, [D$_8$]THF, 23 °C): δ = 3.42 (s, 4 H, DME), 3.26 (s, 6 H, DME), 3.09 [q, 6 H, ^3J = 7.20 Hz, $(CH_3\mathit{C}H_2NC(Me)N\mathit{t}Bu)$], 1.88 [s, 9 H, $(EtNC(\mathit{C}H_3)N\mathit{t}Bu)$], 1.22 [s, 27 H $(EtNC(Me)NC(\mathit{C}H_3)_3)$], 1.02 [t, 9 H, ^3J = 7.20 Hz, $(\mathit{C}H_3CH_2NC(Me)N\mathit{t}Bu)$] ppm. **^{13}C NMR** (100.6 MHz, [D$_8$]toluene, 23 °C): δ = 172.6 $[EtN\mathit{C}(Me)N\mathit{t}Bu]$, 72.7, 58.9 (DME), 51.9 $[EtNC(Me)N\mathit{C}(CH_3)_3]$, 42.6 $[CH_3\mathit{C}H_2NC(Me)N\mathit{t}Bu]$, 32.9 $[EtNC(Me)NC(\mathit{C}H_3)_3]$, 18.0 $[\mathit{C}H_3CH_2NC(Me)N\mathit{t}Bu]$, 15.8 $[EtNC(\mathit{C}H_3)N\mathit{t}Bu]$ ppm. **MS** (EI, 70 eV): *m*/*z* (%) 562 (50) $[La(L)_3]^+$, 421 (100) $[La(L)_2]^+$, 505 (89) $[La(L)_2\{EtNC(Me)N\}]^+$, 405 (83) $[La(L)\{EtNCN\mathit{t}Bu\}]^+$, 389 (79) $[La\{EtNCN\mathit{t}Bu\}_2]^+$, 142 (60) $[L]^+$. **IR** (ATR): $\tilde{\nu}_{max}$ = 3045 (w), 2957 (m, ν_s CH_3), 2930 (m, ν_{as} CH_2), 2904 (m), 2863 (m, $\nu_{as/s}$ CH_3, CH_2), 2836 (m), 2661 (w), 1655 (w, ν NCN), 1615 (w), 1484 (s, $\delta_{as/s}$ CH_3/CH_2), 1406 (s), 1368 (m), 1356 (m, δ_s

CH_3), 1334 (vs, δ_s CH_3), 1276 (m), 1208 (vs), 1149 (m, ν_{as} C-O-C), 1121 (m), 1985 (m), 1029 (m), 980 (m), 910 (w), 871 (w), 812 (m), 783 (w), 758 (m), 635 (m), 615 (w), 569 (m), 535 (m), 472 (m), 439 (w), 340 (m), 220 (vs), 119 (vs), 77 (m) cm^{-1}.

Li(THF)[Ce(L)$_4$] (3): From 0.49 g (1.98 mmol) $CeCl_3$. Yield of pale yellow, block-like crystals: 0.58 g (37 %). M.p. 92 °C (dec.). $C_{36}H_{76}CeLiN_8O$ (784.10 g·mol^{-1}): calcd. C 55.14; H 9.77; N 14.29 %; found: C 54.02; H 9.64; N 15.69 %. **^{1}H NMR** (400.1 MHz, [D$_8$]THF, 23 °C): δ = 3.59 (m, 4 H, THF), 2.60- 3.06 [m, 8 H, (CH_3CH_2NC(Me)N*t*Bu)], 2.60–3.06, 1.10–1.16 [m, 36 H, (EtNC(Me)NC(CH_3)$_3$)], 1.77 (m, 4 H, THF), 0.96, 0.53 [s_{br}, 12 H, EtNC(CH_3)N*t*Bu], –3.56 – (–2.52) (m, 12 H, CH_3CH_2NC(Me)N*t*Bu) ppm. **^{13}C NMR** (100.6 MHz, [D$_8$]toluene, 23 °C): δ = 183.1, 160.6 [EtN*C*(Me)N*t*Bu], 68.1 (THF), 53.8, 51.6 [EtNC(Me)N*C*(CH_3)$_3$], 50.0, 42.6 [CH_3CH_2NC(Me)N*t*Bu], 35.5, 33.8 [EtNC(Me)NC(*C*H_3)$_3$], 30.2, 28.1 [*C*H_3CH_2NC(Me)N*t*Bu], 26.3 (THF), 19.7, 18.6 [EtNC(*C*H_3)N*t*Bu] ppm. **MS** (EI, 70 eV): *m/z* (%) 563 (87) [Ce(L)$_3$]$^+$, 422 (100) [Ce(L)$_2$]$^+$, 142 (88) [L]$^+$. **IR** (ATR): $\tilde{\nu}_{max}$ = 2959 (m, ν_s CH_3), 2921 (m, ν_{as} CH_2), 2861 (m, $\nu_{as/s}$ CH_3/CH_2), 2834 (w), 1494 (vs, $\delta_{as/s}$ CH_3/CH_2), 1410 (s), 1384 (m), 1357 (m, δ_s CH_3), 1332 (s, δ_s CH_3), 1278 (w), 1206 (vs), 1141 (m), 1125 (vs, ν_{as} C-O-C), 1064 (m), 1049 (m), 1029 (m), 1006 (m), 917 (w), 898 (w), 819 (w), 782 (m), 756 (m), 678 (w), 614 (m), 589 (w), 555 (w), 477 (w), 445 (w), 371 (w), 326 (m), 194 (s), 148 (m), 82 (m), 62 (m) cm^{-1}.

Sc(L)$_3$ (4): From 0.93 g (2.64 mmol) $ScCl_3(THF)_{1.8}$. Yield of colorless crystals: 1.0 g (40 %). M.p. 153 °C (dec.). $C_{24}H_{51}N_6Sc$ (468.65 g·mol^{-1}): calcd. C 61.50; H 10.91; N 17.93 %; found: C 61.66; H 11.04; N 18.00 %. **^{1}H NMR** (400.1 MHz, [D$_8$]THF, 23 °C): δ = 3.10 [s_{br}, 6 H, (CH_3CH_2NC(Me)N*t*Bu)], 1.96 [s, 9 H, (EtNC(*C*H_3)N*t*Bu)], 1.24 [s, 27 H, (EtNC(Me)NC(*C*H_3)$_3$),], 0.98 [t, 9 H, ^3J = 7.20 Hz, (*C*H_3CH_2NC(Me)N*t*Bu)] ppm. **^{13}C NMR** (100.6 MHz, [D$_8$]toluene, 23 °C): δ = 175.2 [EtN*C*(Me)N*t*Bu], 51.7 [EtNC(Me)N*C*(CH_3)$_3$], 41.9 [CH_3CH_2NC(Me)N*t*Bu], 33.0 [EtNC(Me)NC(*C*H_3)$_3$], 18.0 [*C*H_3CH_2NC(Me)N*t*Bu], 14.8 [EtNC(*C*H_3)N*t*Bu] ppm. **^{45}Sc NMR** (97.2 MHz, [D$_8$]THF, 23 °C): δ = 208 ppm. **MS** (EI, 70 eV): *m/z* (%) 468 (17) [M]$^+$, 411 (22) [Sc(L)$_2${EtNC(Me)N}]$^+$, 327 (80) [Sc(L)$_2$]$^+$, 142 (100) [L]$^+$, 127 (80) [EtNCN*t*Bu]$^+$. **IR** (ATR): $\tilde{\nu}_{max}$ = 2962 (m, ν_s CH_3), 2926 (m, ν_{as} CH_2), 2902 (m), 2859 (m, $\nu_{as/s}$ CH_3/CH_2), 2665 (w), 1491 (vs, $\delta_{as/s}$ CH_3/CH_2), 1433 (s), 1412 (vs), 1358 (m, δ_s CH_3), 1336 (vs, δ_s CH_3), 1279 (w), 1228 (s), 1214 (vs), 1165 (s), 1135 (m), 1090 (m), 1070 (m), 1032 (m), 1016 (m), 982 (m), 914 (w), 880 (w), 819 (m), 783 (m), 766 (m), 635 (m), 619 (m), 575 (m), 557 (m), 476 (m), 440 (m), 370 (vs, ν Sc-N), 296 (m), 220 (m), 184 (m), 135 (m), 119 (m), 78 (m), 68 (m) cm^{-1}.

Ho(L)$_3$ (5): From 0.72 g (2.64 mmol) $HoCl_3$. Yield of pale yellow, rod-like crystals: 0.49 g (32 %). M.p. 106 °C. $C_{24}H_{51}HoN_6$ (588.64 g·mol^{-1}): calcd. C 48.97; H 8.73; N 14.28 %; found: C 49.07; H 8.85; N 14.88 %. Due to the strongly paramagnetic character of the Ho^{3+} ion no meaningful NMR spectroscopic data could be obtained for **5**. **MS** (EI, 70 eV): *m/z* (%) 588 (16) [M]$^+$, 531 (73) [Ho(L)$_2${EtNC(Me)N}]$^+$, 447 (52) [Ho(L)$_2$]$^+$, 142 (96) [L]$^+$, 127 (86) [EtNCN*t*Bu]$^+$, 86 (100) [EtNC(Me)N]$^+$. **IR** (ATR): $\tilde{\nu}_{max}$ = 2959 (m, ν_s CH_3), 2928 (m, ν_{as} CH_2), 2904 (m), 2861 (m, $\nu_{as/s}$ CH_3/CH_2), 1644 (w, ν NCN), 1487 (vs, $\delta_{as/s}$ CH_3/CH_2), 1410 (vs), 1372 (m), 1357 (m, δ_s CH_3), 1336 (vs, δ_s CH_3), 1275 (w), 1226 (s), 1212 (vs), 1158 (m), 1134 (m), 1089 (w), 1031 (m), 1016 (m), 981 (w), 879 (w), 816 (m), 784 (m), 763 (m), 636 (m), 617 (m), 573 (m), 539 (w), 475 (w), 440 (w), 342 (m), 226 (m), 130 (m), 96 (m), 54 (m) cm^{-1}.

Acknowledgements

General financial support of this work by the Otto-von-Guericke-Universität Magdeburg is gratefully acknowledged.

Keywords: Amidinate; Lanthanides; Cerium; Structure elucidation

References

[1] P. J. Bailey, S. Pace, *Coord. Chem. Rev.* **2001**, *214*, 91–141.
[2] D. A. Kissounko, M. V. Zabalov, G. P. Brusova, D. A. Lemenovskii, *Russ. Chem. Rev.* **2006**, *75*, 351–374.
[3] P. C. Junk, M. L. Cole, *Chem. Commun.* **2007**, 1579–1590.
[4] F. T. Edelmann, *Adv. Organomet. Chem.* **2008**, *57*, 183–352.
[5] C. E. Hayes, D. B. Leznoff, *Coord. Chem. Rev.* **2014**, *266–267*, 155–170.
[6] Y.-Y. Zhang, Y.-J. Lin, X.-C. Shi, G.-X. Jin, *Pure Appl. Chem.* **2014**, *86*, 953–965.
[7] T. Chlupatý, A. Růžička, *Coord. Chem. Rev.* **2016**, *314*, 103–113.
[8] G. B. Deacon, M. E. Hossain, P. C. Junk, M. Salehisaki, *Coord. Chem. Rev.* **2017**, *340*, 247–265.
[9] F. T. Edelmann, *Chem. Soc. Rev.* **2009**, *38*, 2253–2268.
[10] F. T. Edelmann, *Chem. Soc. Rev.* **2012**, *41*, 7657–7672.
[11] H. Nagashima, H. Kondo, T. Hayashida, Y. Yamaguchi, M. Gondo, S. Masuda, K. Miyazaki, K. Matsubara, K. Kirchner, *Coord. Chem. Rev.* **2003**, *245*, 177–190.
[12] F. T. Edelmann, *Struct. Bonding (Berlin)* **2010**, *137*, 109–163.
[13] S. Collins, *Coord. Chem. Rev.* **2011**, *255*, 118–138.
[14] T. Elkin, M. S. Eisen, *Catal. Sci. Technol.* **2015**, *5*, 82–95.
[15] G. von Doremaele, M. van Duin, M. Valla, A. Berthoud, *J. Polym. Sci. A: Polym. Chem.* **2017**, *55*, 2877–2891.
[16] B. S. Lim, A. Rahtu, J.-S. Park, R. G. Gordon, *Inorg. Chem.* **2003**, *42*, 7951–7958.
[17] Z. Li, S. T. Barry, R. G. Gordon, *Inorg. Chem.* **2005**, *44*, 1728–1735.
[18] D. Rische, H. Parala, A. Baunemann, T. Thiede, R. Fischer, *Surf. Coat. Technol.* **2007**, *201*, 9125–9130.
[19] K. Xu, A. R. Chaudhuri, H. Parala, D. Schwendt, T. de los Arcos, H. J. Osten, A. Devi, *J. Mater. Chem. C: Mater. Opt. Electr. Dev.* **2013**, *1*, 3939–3946.
[20] A. Devi, *Coord. Chem. Rev.* **2013**, *257*, 3332–3384.
[21] A. Kurek, P. G. Gordon, S. Karle, A. Devi, S. T. Barry, *Aust. J. Chem.* **2014**, *67*, 989–996.
[22] P. G. Gordon, A. Kurek, S. T. Barry, *ECS J. Solid State Sci. Technol.* **2015**, *4*, N3188–N3197.
[23] L. Mai, Z. Giedraityte, M. Schmidt, D. Rogalla, S. Scholz, A. D. Wieck, A. Devi, *J. Mater. Sci.* **2017**, *52*, 6216–6224.
[24] M. Lukas, N. Boysen, E. Subasi, T. de los Arcos, D. Rogalla, G. Grundmeier, C. Bock, H.-L. Lu, A. Devi, *RSC Adv.* **2018**, *8*, 4987–4994.
[25] T. Chen, C. Xu, T. H. Baum, G. T. Stauf, J. F. Roeder, A. G. DiPasquale, A. L. Rheingold, *Chem. Mater.* **2010**, *22*, 27.
[26] Z. Li, D. K. Lee, M. Coulter, L. N. J. Rodriguez, R. G. Gordon, *Dalton Trans.* **2008**, 2592.
[27] M. Krasnopolski, C. G. Hrib, R. W. Seidel, M. Winter, H.-W. Becker, D. Rogalla, R. A. Fischer, F. T. Edelmann, A. Devi, *Inorg. Chem.* **2013**, *52*, 286.
[28] A. Schmielau, C. G. Hrib, V. Lorenz, L. Hilfert, F. Zörner, S. Busse, F. T. Edelmann, *J. Organomet. Chem.* **2015**, *791*, 252–257.
[29] R. D. Shannon, *Acta Crystallogr., Sect. A* **1976**, *32*, 751–767.
[30] P. Tutacz, N. Harmgarth, F. Zörner, P. Liebing, L. Hilfert, S. Busse, F. T. Edelmann, *Z. Anorg. Allg. Chem.* **2018**, *644*, 1653–1659.
[31] C. R. Groom, F. H. Allen, *Angew. Chem. Int. Ed.* **2014**, *53*, 662–671.

[32] F. M. Sroor, C. G. Hrib, L. Hilfert, S. Busse, F. T. Edelmann, *New J. Chem.* **2015**, *39*, 7595–7601.
[33] R. Anwander, M. Dolg, F. T. Edelmann, *Chem. Soc. Rev.* **2017**, *46*, 6697–6709.
[34] S. Barroso, J. Cui, J. M. Carretas, A. Cruz, I. C. Santos, M. T. Duarte, J. P. Telo, N. Marques, A. M. Martins, *Organometallics* **2009**, *28*, 3449–3458.
[35] C.-L. Pan, S.-D. Sheng, J. Wang, Y.-S. Pan, *Mendeleev Commun.* **2011**, *21*, 318–319.
[36] X. Lu, M.-T. Ma, Y.-M. Yao, Y. Zhang, Q. Shen, *Inorg. Chem. Commun.* **2010**, *13*, 1566–1568.
[37] H. Yin, P. J. Carroll, B. C. Manor, J. M. Anna, E. J. Schelter, *J. Am. Chem. Soc.* **2016**, *138*, 5984–5993.
[38] M. P. Coles, P. B. Hitchcock, A. V. Khvostov, M. F. Lappert, Z. Li, A. V. Protchenko, *Dalton Trans.* **2010**, *39*, 6780–6788.
[39] T. Mehdoui, J. C. Berthet, P. Thuery, M. Ephritikhine, *CSD Communication*, CCDC 958641, **2013**.
[40] F. M. Sroor, C. G. Hrib, L. Hilfert, P. G. Jones, F. T. Edelmann, *J. Organomet. Chem.* **2015**, *785*, 1–10.
[41] P. Dröse, C. G. Hrib, L. Hilfert, F. T. Edelmann, *Z. Anorg. Allg. Chem.* **2011**, *637*, 31–33.
[42] A. L. Spek, *Acta Crystallogr., Sect. C* **2015**, *71*, 8–18.
[43] J. H. Freeman, M. L. Smith, *J. Inorg. Nucl. Chem.* **1958**, *7*, 224–227.
[44] Stoe & Cie **2002**, *X-Area and X-Red*, Stoe & Cie, Darmstadt, Germany.
[45] G. M. Sheldrick, *Acta Crystallogr., Sect. A* **2015**, *71*, 3–8.
[46] G. M. Sheldrick, *Acta Crystallogr., Sect. C* **2015**, *71*, 3–8.

Received: July 1, 2019

